

Organosilane surfactant-directed synthesis of hierarchical porous SAPO-34 catalysts with excellent MTO performance†

Cite this: DOI: 10.1039/c4cc02050b

Received 19th March 2014,
Accepted 30th April 2014

DOI: 10.1039/c4cc02050b

www.rsc.org/chemcomm

Qiming Sun,^a Ning Wang,^a Dongyang Xi,^a Miao Yang^b and Jihong Yu*^a

Using an organosilane surfactant as the mesopore director, hierarchical porous silicoaluminophosphate SAPO-34 is obtained as an assembly of nanocrystallites intergrown into cubic micrometer-sized crystals, which show excellent performance in MTO reactions with a remarkably prolonged catalyst lifetime and enhanced selectivity of ethylene and propylene compared to the conventional microporous SAPO-34.

Zeolites are the most widely used solid catalysts in industry due to their microporous structures and the resulting unique shape selectivity.¹ Silicoaluminophosphate molecular sieve SAPO-34 with the topological structure of **CHA** has been intensively studied as one of the most excellent catalysts for the methanol-to-olefin (MTO) conversion. Such an MTO process provides an alternative route to produce light olefins from nonpetroleum sources, and has gained considerable attention in the last three decades.² SAPO-34 with a large **CHA** cage (9.4 Å in diameter) and small 8-ring pore (0.38 Å × 0.38 Å) opening,³ as well as mild acidity can induce a high selectivity of ethylene and propylene in MTO reactions. However, the large **CHA** cage and narrow pore opening also cause the problem of rapid deactivation due to the limitation of mass transport and a large amount of organic species accommodating in the large cavities during methanol conversion.⁴ Hence, overcoming the inherent diffusion limitations and retarding coke deposition are of significance to prolong the catalytic activity. So far, various approaches have been developed to reduce the coke deposition, such as optimizing the synthesis conditions,⁵ modifying the

catalyst acidity,⁶ and decreasing the crystal size.⁷ Another synthetic strategy is the introduction of meso- or/and macropores into the microporous zeolite crystals to obtain a hierarchical structure.⁸ In recent decades, some methods have been successfully employed for the preparation of hierarchical porous aluminosilicate zeolites, such as the post-treatment method,⁹ the hard-templating method,¹⁰ and the soft-templating method.¹¹ Notably, Ryoo's group demonstrated the soft-templating synthesis of zeolites by introducing organosilane surfactants as the mesopore director into conventional zeolite synthesis compositions.¹² They further extended this strategy to the synthesis of mesoporous aluminophosphate molecular sieves.¹³ Inspired by this design concept, a few attempts have been made to synthesize hierarchical porous silicoaluminophosphate molecular sieves with the assistance of organosilane surfactants.¹⁴ However, the synthesis of hierarchical porous SAPO-34 catalysts with excellent MTO catalytic performance by using this method has seen less success.¹⁵

In this work, the hierarchical porous SAPO-34 catalysts were successfully synthesized using [3-(trimethoxysilyl)propyl]-octadecyldimethyl-ammonium chloride (TPOAC) as the mesopore director through a one-step hydrothermal crystallization. The hierarchical porous SAPO-34 catalysts were prepared as cubic agglomerates of small nanocrystals, which exhibit a remarkably prolonged catalytic lifetime and excellent light olefin selectivity in the MTO conversions compared with the conventional microporous SAPO-34 catalyst synthesized without adding organosilane surfactants.

The hierarchical porous SAPO-34 catalysts (S_{H1} and S_{H2}) were synthesized from the starting gels with the optimized molar compositions of 1.0Al₂O₃: 1.0P₂O₅: 3.0Mor: 0.6SiO₂: 80H₂O: x TPOAC ($x = 0.1$ and 0.15) under hydrothermal conditions at 180 °C by using morpholine (Mor) as the template for micropores and TPOAC for mesopores. As a comparison, the conventional microporous SAPO-34 (S_M) was synthesized under the same synthesis conditions without the addition of TPOAC.

The XRD patterns of all samples show typical diffraction peaks of the **CHA** structure (Fig. 1), proving the phase purity of

^a State Key Laboratory of Inorganic Synthesis and Preparative Chemistry, College of Chemistry, Jilin University, Changchun 130012, P. R. China. E-mail: jihong@jlu.edu.cn

^b National Engineering Laboratory for Methanol to Olefins, Dalian National Laboratory for Clean Energy, Dalian Institute of Chemical Physics, Chinese Academy of Sciences, Dalian 116023, P. R. China

† Electronic supplementary information (ESI) available: More details of experimental and characterization processes, TEM, DFT pore distribution, FT-IR, TG-DTA, ³¹P, ²⁷Al, ¹H and ²⁹Si MAS NMR, NH₃-TPD, and the MTO reaction catalytic results. See DOI: 10.1039/c4cc02050b

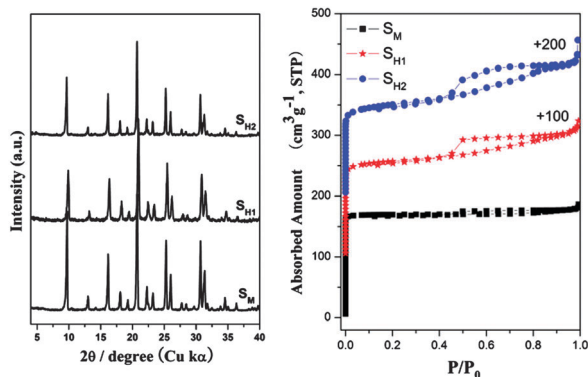


Fig. 1 XRD patterns (left) and N_2 adsorption–desorption isotherms (right) of conventional microporous SAPO-34 (S_M) and hierarchical porous SAPO-34 (S_{H1} and S_{H2}).

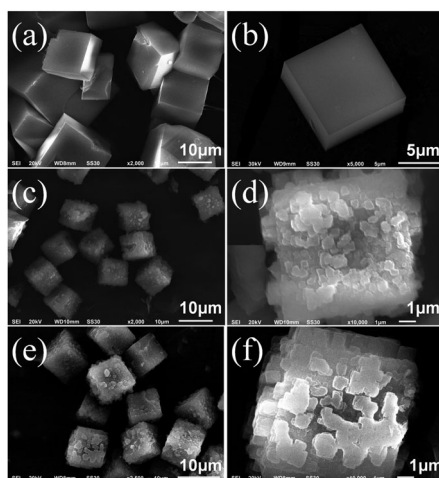


Fig. 2 SEM images of conventional microporous SAPO-34 (S_M) (a, b) and hierarchical porous SAPO-34 (S_{H1}) (c, d) and S_{H2} (e, f).

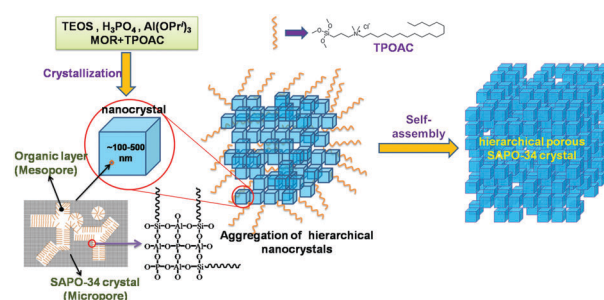
as-synthesized SAPO-34. Their SEM images show the characteristic cubic morphology of the CHA crystals (Fig. 2). Notably, different from the conventional microporous SAPO-34 (S_M) with a smooth crystal surface, samples S_{H1} and S_{H2} are observed to be an aggregation of small cubic-like nanocrystals.

The size of the individual nanocrystals ranges from 100 to 500 nm. The TEM images of samples S_{H1} and S_{H2} clearly reveal the existence of small mesopores (2–5 nm) and larger mesopores (ca. 30 nm) in the nanocrystalline domains (Fig. S1, ESI†). In contrast to conventional microporous SAPO-34 (S_M) showing

the type-I N_2 adsorption–desorption isotherms, samples S_{H1} and S_{H2} exhibit the type-IV isotherms, and the large hysteresis loops in the region $0.4 < P/P_0 < 0.9$ are observed due to the capillary condensation in the mesopores (Fig. 1).¹³ Particularly, sample S_{H2} exhibits a significantly increased external surface area ($123.6 \text{ m}^2 \text{ g}^{-1}$) and mesopore volume ($0.26 \text{ cm}^3 \text{ g}^{-1}$) as compared with the conventional microporous SAPO-34. Meanwhile, the pore size distribution also demonstrates the existence of hierarchical porosity in samples S_{H1} and S_{H2} (Fig. S2, ESI†). The detailed surface area and pore volume data are summarized in Table 1.

The FT-IR spectra further confirm the existence of the TPOAC surfactant in the hierarchical porous SAPO-34 crystals (Fig. S3, ESI†). Different from microporous SAPO-34 (S_M), the sharp IR peaks at 2922 cm^{-1} and 2855 cm^{-1} exist in samples S_{H1} and S_{H2} , which are ascribed to the vibration of the C–H bond derived from the hydrophobic alkyl chain of the TPOAC surfactant.¹⁶ Elemental analyses show that the C/N ratios of samples S_M , S_{H1} and S_{H2} are increased due to the introduction of the TPOAC surfactant (Table 1). In addition, the TG-DTA analyses also demonstrate that the TPOAC surfactants are occluded into the hierarchical porous SAPO-34 crystals (Fig. S4, ESI† and Table 1). The hierarchical porous SAPO-34 samples have more weight loss and the exothermic peak at $340 \text{ }^\circ\text{C}$ is distinct due to the thermal decomposition of the TPOAC surfactant.

It is believed that the introduction of an organosilane surfactant plays an important role in the formation of hierarchical porous SAPO-34. The proposed assembly pathway of nanocrystallites into micrometer-sized hierarchical porous SAPO-34 crystals is shown in Scheme 1. The silica portion of the TPOAC



Scheme 1 Proposed assembly pathway of cubic hierarchical porous SAPO-34 crystals aggregated by small cubic nanocrystals assisted by the organosilane surfactant.

Table 1 Compositions and textural properties of conventional microporous SAPO-34 (S_M) and hierarchical porous SAPO-34 (S_{H1} and S_{H2}) catalysts

Sample no.	Molar composition ^a	TG ^b (%)	C/N ^c	S_{BET}^d ($\text{m}^2 \text{ g}^{-1}$)	S_{micro}^e ($\text{m}^2 \text{ g}^{-1}$)	S_{ext}^e ($\text{m}^2 \text{ g}^{-1}$)	V_{micro}^e ($\text{cm}^3 \text{ g}^{-1}$)	V_{meso}^f ($\text{cm}^3 \text{ g}^{-1}$)
S_M	$\text{Si}_{0.18}\text{Al}_{0.45}\text{P}_{0.37}\text{O}_2$	20.42	3.95	562.1	551.2	10.9	0.26	0.04
S_{H1}	$\text{Si}_{0.17}\text{Al}_{0.45}\text{P}_{0.38}\text{O}_2$	22.27	5.20	525.4	441.7	83.7	0.21	0.17
S_{H2}	$\text{Si}_{0.16}\text{Al}_{0.46}\text{P}_{0.38}\text{O}_2$	25.05	5.85	507.9	384.3	123.6	0.18	0.26

^a Measured by inductively coupled plasma (ICP). ^b Weight loss of templates (%) measured by TG-DTA (Fig. S4, ESI). ^c C/N of templates measured using an element analyzer. ^d S_{BET} (total surface area) calculated by applying the BET equation using the linear part ($0.05 < P/P_0 < 0.30$) of the adsorption isotherm. ^e S_{micro} (micropore area), S_{ext} (external surface area) and V_{micro} (micropore volume) calculated using the t -plot method. ^f V_{meso} (mesopore volume) calculated using the BJH method (from desorption).

surfactant is firstly incorporated into the resultant silicoaluminophosphate framework, and the organic tails of the TPOAC surfactant forming the organic layers direct the mesoporous structure. Meanwhile, the organic tails of the TPOAC surfactant attached on the surface of nanocrystals provide a capping effect,^{12b} thus limiting the further growth of the nanocrystals, forming the cubic-like agglomerates with some intervoid space.

The solid-state ³¹P, ²⁷Al, ¹H, and ²⁹Si MAS NMR spectra of calcined SAPO-34 samples are presented in Fig. S5 (ESI†). Compared with the conventional microporous SAPO-34, the hierarchical porous SAPO-34 crystals show more pentacoordinated and octahedral aluminum atoms attributed to the extra-framework aluminum species in the formation of hierarchical structure.¹⁷

Inductively coupled plasma (ICP) analyses show that all samples have similar molar compositions (Table 1). It is noticed that with the increase of the TPOAC surfactant, the silicon contents of samples decrease slightly from S_M, S_{H1} to S_{H2}. This may be because the increased steric hindrance caused by the mutual repulsion of surfactant decreases the incorporation of silicon into the frameworks. Meanwhile, NH₃-TPD analyses reveal that the introduction of the TPOAC surfactant can also affect the acidity of catalysts (Fig. S6, ESI†). The hierarchical porous SAPO-34 samples have lower acidic strength and acidic concentration in strong acid sites compared with the conventional microporous SAPO-34. Furthermore, S_{H2} has the lowest acidic strength and acidic concentration in strong acid sites that is connected with the increased amount of TPOAC and the decreased silicon content in the framework.

Catalytic tests of methanol conversion were carried out at 673 K in a fixed-bed reactor over the catalysts. Significantly, the hierarchical porous SAPO-34 catalysts exhibit a remarkably prolonged catalyst lifetime and enhanced light olefin selectivity compared with the conventional microporous SAPO-34 catalyst (Fig. 3, Table S1, ESI†). The yields of products of samples S_M, S_{H1} and S_{H2} are shown in Fig. S7–S9 (ESI†). Particularly, the lifetime of sample S_{H2} (466 min) with hierarchical porous structure is more than four-times higher than that of S_M (106 min) with only microporous structure. Meanwhile, the selectivity of ethylene and propylene of sample S_{H2} reaches up to 82.7%, which has improved more than 10% compared with

sample S_M (71.9%) (Table S1, ESI†). The prominent difference in the catalytic performance of hierarchical porous SAPO-34 and conventional microporous SAPO-34 catalysts can be explained by the difference in the level of porosity, acidity, as well as crystallite size. The generated mesopore in the hierarchical porous SAPO-34 can greatly enhance the transfer of the reaction products from the narrow pore to outside space and reduce the coke formation and thus prolong the lifetime. Furthermore, the decreased acidic strength and acidic concentration of hierarchical porous SAPO-34 catalysts can also retard the coke formation and thus prolong the catalyst lifetime.⁶ Hydrogen transfer index (HTI, C₃H₈/C₃H₆) indicates that the hierarchical porous SAPO-34 catalysts can decrease the hydrogen transfer level of secondary transformation of olefin products and lower the coking rate (Fig. S10 and Table S2, ESI†), especially, sample S_{H2} exhibits the lowest coking rate of 0.132 mg min⁻¹, which is only about 40% of sample S_M. In addition, the decreased nanocrystallite size in the agglomerates of the hierarchical porous SAPO-34 catalysts is also an important reason for enhancing the lifetime.⁷ The smaller crystals can shorten the diffusion length reactant and generated products and greatly enhance the mass transfer during the methanol conversion, and thus prolong the lifetime.¹⁸

In summary, hierarchical porous silicoaluminophosphate SAPO-34 catalysts have been successfully synthesized using the organosilane surfactant as the mesopore director by direct hydrothermal crystallization. The hierarchical porous SAPO-34 crystals are obtained as cubic aggregates of nanocrystallites. Thanks to the hierarchical porosity, decreased acidity as well as reduced nanocrystallite size, the hierarchical porous SAPO-34 catalysts exhibit four-times prolonged catalytic lifetime and more than 10% improvement of light olefin (C₂H₄ + C₃H₆) selectivity in MTO conversion compared with the conventional microporous SAPO-34 catalyst. This work demonstrates an effective organosilane surfactant-directed approach to prepare hierarchical porous silicoaluminophosphate molecular sieves with improved catalytic properties.

We thank the State Basic Research Project of China (Grant No. 2011CB808703 and 2014CB931802), National Natural Science Foundation of China (Major Program, Grant No. 91122029) and the Major International Joint Research Project of China for financial support (Grant No. 21320102001).

Notes and references

- (a) A. Corma, *Chem. Rev.*, 1995, **95**, 559; (b) A. Corma, *Chem. Rev.*, 1997, **97**, 2373; (c) Z. Wang, J. Yu and R. Xu, *Chem. Soc. Rev.*, 2012, **41**, 1729.
- (a) C. D. Chang, *Catal. Rev.*, 1983, **25**, 1; (b) U. Olsbye, S. Svelle, M. Bjørgen, P. Beato, T. V. W. Janssens, F. Joensen, S. Bordiga and K. P. Lillerud, *Angew. Chem., Int. Ed.*, 2012, **51**, 5810.
- B. M. Lok, C. A. Messina, R. L. Patton, R. T. Gajek, T. R. Cannan and E. M. Flanigen, *J. Am. Chem. Soc.*, 1984, **106**, 6092.
- D. Chen, K. Moljord and A. Holmen, *Microporous Mesoporous Mater.*, 2012, **164**, 239.
- (a) S. Lin, J. Li, R. Sharma, J. Yu and R. Xu, *Top. Catal.*, 2010, **53**, 1304; (b) S. Askari and R. Halladj, *Ultrason. Sonochem.*, 2012, **19**, 554.
- M. Kang and T. Inui, *Catal. Lett.*, 1998, **53**, 171.
- (a) G. Yang, Y. Wei, S. Xu, J. Chen, J. Li, Z. Li, J. Yu and R. Xu, *J. Phys. Chem. C*, 2013, **117**, 8214; (b) M. Yang, P. Tian, C. Wang, Y. Yuan, Y. Yang, S. Xu, Y. He and Z. Liu, *Chem. Commun.*, 2014, **50**, 1845.

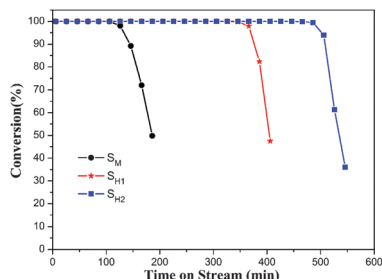


Fig. 3 Methanol conversion variation with time-on-stream over conventional microporous SAPO-34 (S_M) and hierarchical porous SAPO-34 (S_{H1} and S_{H2}) catalysts. Experimental conditions: WHSV = 2 h⁻¹, T = 673 K, catalyst weight = 300 mg.

- 8 (a) L.-H. Chen, X.-Y. Li, J. C. Rooke, Y.-H. Zhang, X.-Y. Yang, Y. Tang, F.-S. Xiao and B.-L. Su, *J. Mater. Chem.*, 2012, **22**, 17381; (b) V. Valtchev, G. Majano, S. Mintova and J. Perez-Ramirez, *Chem. Soc. Rev.*, 2013, **42**, 263; (c) H. Yang, Z. Liu, H. Gao and Z. Xie, *J. Mater. Chem.*, 2010, **20**, 3227; (d) F. Schmidt, C. Hoffmann, F. Giordanino, S. Bordiga, P. Simon, W. Carrillo-Cabrera and S. Kaskel, *J. Catal.*, 2013, **307**, 238.
- 9 L. Sommer, D. Mores, S. Svelle, M. Stöcker, B. M. Weckhuysen and U. Olsbye, *Microporous Mesoporous Mater.*, 2010, **132**, 384.
- 10 C. J. H. Jacobsen, C. Madsen, J. Houzvicka, I. Schmidt and A. Carlsson, *J. Am. Chem. Soc.*, 2000, **122**, 7116.
- 11 L. Wu, V. Degirmenci, P. C. M. M. Magusin, B. M. Szyja and E. J. M. Hensen, *Chem. Commun.*, 2012, **48**, 9492.
- 12 (a) M. Choi, H. S. Cho, R. Srivastava, C. Venkatesan, D.-H. Choi and R. Ryoo, *Nat. Mater.*, 2006, **5**, 718; (b) C. Jo, J. Jung, H. S. Shin, J. Kim and R. Ryoo, *Angew. Chem.*, 2013, **125**, 10198.
- 13 M. Choi, R. Srivastava and R. Ryoo, *Chem. Commun.*, 2006, 4380.
- 14 J.-Y. Kim, J. Kim, S.-T. Yang and W.-S. Ahn, *Fuel*, 2013, **108**, 515.
- 15 S.-T. Yang, J.-Y. Kim, H.-J. Chae, M. Kim, S.-Y. Jeong and W.-S. Ahn, *Mater. Res. Bull.*, 2012, **47**, 3888.
- 16 G. Liu, P. Tian, J. Li, D. Zhang, F. Zhou and Z. Liu, *Microporous Mesoporous Mater.*, 2008, **111**, 143.
- 17 (a) S. Ashtekar, S. V. V. Chilukuri and D. K. Chakrabarty, *J. Phys. Chem.*, 1994, **98**, 4878; (b) A. M. Prakash and S. Unnikrishnan, *J. Chem. Soc., Faraday Trans.*, 1994, **90**, 2291.
- 18 Y. Hirota, K. Murata, M. Miyamoto, Y. Egashira and N. Nishiyama, *Catal. Lett.*, 2010, **140**, 22.